land

MDPI

Article

Distinguishing Geogenic Load and Anthropogenic Contribution to Soil Contamination in Mineralised Mountain Landscape of Ore Mountains (Czech Republic) Using Cumulative Distribution Functions

Michal Hošek *, Petra Pavlíková, Matěj Šoltýs, Štěpánka Tůmová and Tomáš Matys Grygar

Faculty of Environment, Jana Evangelisty Purkyně University in Ústí nad Labem, 400 96 Ústí nad Labem, Czech Republic; grygart@ujep.cz (T.M.G.)
* Correspondence: michal.hosek@ujep.cz

Abstract: In ore regions impacted by mining and metal smelting emissions, distinguishing between geogenic anomalies and anthropogenic contamination poses a significant challenge. In a study from two areas with different mining histories in the Ore Mountains, Czech Republic, we demonstrate that sampling of topsoils and subsoils respecting local geology and correct soil data treatment respecting soil textural variability effects are indispensable to the correct construction and interpretation of geochemical maps and identification of anthropogenic contamination by As, Cu, Pb, and Zn. The list of analysed elements must include both potentially toxic and lithogenic elements, otherwise natural controls of soil composition cannot be deciphered. By using empirical cumulative distribution functions, we found that local backgrounds for As/Fe and Pb/Ti are naturally elevated (5.7 to 9.8 times and 2.1 to 2.7 times higher, respectively) compared to the global averages. We constructed geochemical maps with topsoil minus subsoil concentrations to show the main directions of spreading anthropogenic contamination. The anthropogenic diffuse contamination contribution was calculated and expressed as an enrichment relative to the local background (16% and 12% for As/Fe and 17% and 14% for Pb/Ti, respectively). This corresponds to topsoil enrichment by ca. 15 and 14 mg kg^{-1} for As and ca. 35 and 42 mg kg^{-1} for Pb in the two study areas. The obtained estimates were comparable to the results from the local peat archives. The approach we used is efficient in deciphering natural and anthropogenic controls of PTEs in geochemically complicated areas.

Keywords: geochemical mapping; topsoils; geogenic anomalies; ore region; diffuse contamination; empirical cumulative distribution function; potential toxic elements; soil contamination

check for updates

Citation: Hošek, M.; Pavlíková, P.; Šoltýs, M.; Tůmová, Š.; Matys Grygar, T. Distinguishing Geogenic Load and Anthropogenic Contribution to Soil Contamination in Mineralised Mountain Landscape of Ore Mountains (Czech Republic) Using Cumulative Distribution Functions. *Land* **2024**, *13*, 218. https://doi.org/10.3390/land13020218

Academic Editors: Gregorio García, Rocio Millan and Araceli Pérez-Sanz

Received: 29 December 2023
Revised: 26 January 2024
Accepted: 1 February 2024
Published: 9 February 2024

Copyright: © 2024 by the authors. Licensee MDPI, Basel, Switzerland. This article is an open access article distributed under the terms and conditions of the Creative Commons Attribution (CC BY) license (https://creativecommons.org/licenses/by/4.0/).

1. Introduction

Soil and water contamination is of global concern for its far-reaching consequences for human health. Concentrations of potentially toxic elements (PTE) in soils are mainly analysed to judge food production safety and identify possible anthropogenic contamination [1–5]. Agricultural land is the basis of food production and plays a crucial role everywhere in the world. Increasing industrial and communal soil contamination deteriorates soil quality and has become a major global problem [6,7]. Soil contamination, i.e., PTEs exceeding common background and potentially endangering food production safety, most commonly caused by industrial activities, can also occur naturally in areas with anomalous soil-forming bedrock [4,8–10]. In geochemically anomalous areas, particularly in ore regions with historical mining and smelting [1,2], distinguishing between geogenic anomalies and anthropogenic contamination needs substantial methodologic improvements of current approaches. The study area of this paper, the Ore Mountains of the Czech Republic and Germany, is appropriate for proposing such methodological improvements. The history of mining and smelting in the Ore Mountains started more than 1500 years

ago [11] and both industries have contributed to naturally elevated concentrations of hazardous elements such as As, Pb, and Zn in the environment [12,13]; their consequences are a pertinent problem for local soils and water also at present [14,15]. Simultaneously, the local rocks are anomalous due to geochemical haloes around abundant rock veins, which causes highly elevated PTE contents also in deep soil strata not affected by anthropogenic activities. Despite preceding extensive research, geogenic and anthropogenic contributions to local soils in the Ore Mountains have not been distinguished [2,14].

Interpreting high soil PTE concentrations always requires corrections for the variability of real controlling factors (RCFs) behind soil composition, i.e., a suite of geological, geographic, paedogenic, climatic, and anthropogenic factors affecting soil depth profiles of PTEs [16–19]. All RCFs (Figure 1) cannot be deciphered completely for each soil profile in any study area in the frame of common geochemical mapping projects; there are only individual exceptions of including their substantial portion in specific case studies [1,8,19]. It is thus essential to interpret the soil geochemical datasets in smaller areas, assuming local RCFs are homogeneous in the entire area [18,20,21], and each case study must be conducted using more detailed approaches than common soil monitoring [19]. A holistic approach and geochemical expertise are needed in data interpretation, whenever unbiased and empirically verifiable results are desired [8,9,18,21]. This is certainly a more appropriate approach than the black box data analysis, so often seen (and increasingly popular) today [22], with geochemical soil data mimicking [10,23] instead of understanding and explaining.

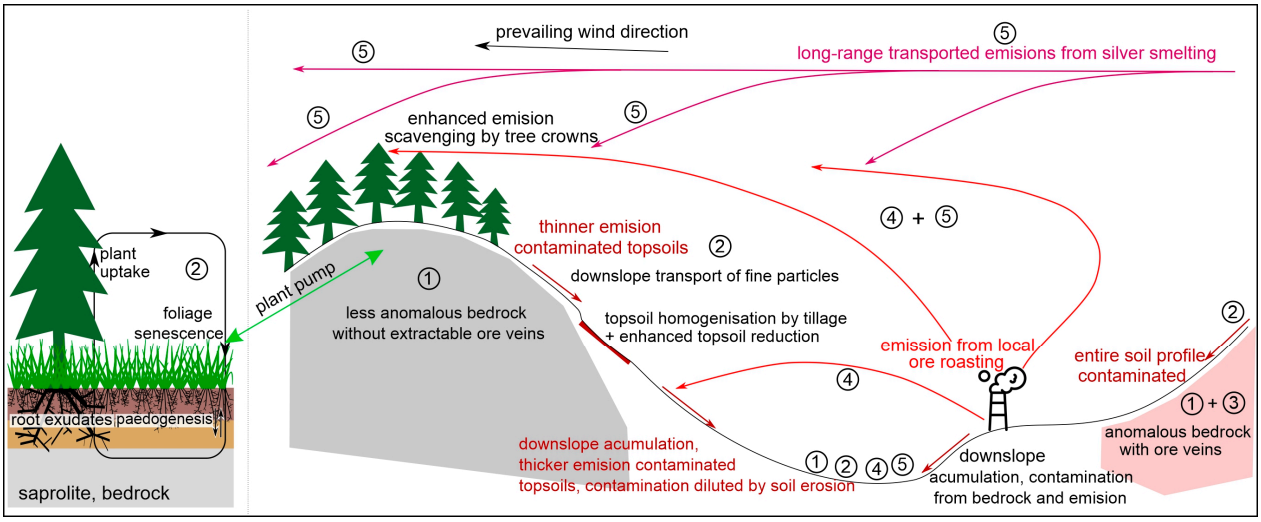


Figure 1. Diagram of real control factors of PTE concentration: (1) bedrock geology; (2) soil processes including soil transport (erosion/accumulation), particle translocations, organic matter enrichment in topsoils, and plant pump [16]; (3) local geogenic anomalies, such as ore veins; (4) localised emissions impacting minor part of soil samples in target area; and (5) diffuse emissions, impacting majority or all soil samples in target area.

In soil studies, geogenic and anthropogenic anomalies, including point and diffuse contamination, can be distinguished using sedimentological tools [24], examination of the entire soil profiles [19,25], or at least a comparison of topsoils (typically 0–20 cm) and subsoils (typically 40–80 cm) [5,10,17,26,27], as a surrogate for complete depth profile analyses. The comparison of topsoils and subsoils can produce hints to help decipher the manifestation of some RCFs, in particular geogenic and emission contamination of soils. The best-performing tools for RCFs deciphering from geochemical datasets are exploratory data analyses (EDA), such as data post-stratification and examination of data series distribution [18]. Empirical cumulative distribution function (ECDF) belongs to the most efficient ways of the visualisation and interpretation of geochemical data series [17,18,28]. Recently, ECDFs have been proposed for the identification of diffuse contamination, deciphering

which is a pertinent challenge in environmental geochemistry due to the inevitable lack of clear definition of outliers in large soil datasets with weak contamination [17,29–31]. The diffuse contamination is, however, dangerous because of the chronic effects of relatively small doses of a contaminant on more components of the soil environment, and hence on the whole ecosystem [32]. Comparison of ECDFs of PTEs and lithogenic element concentrations in topsoils and subsoils was employed for distinguishing natural topsoil enrichment, point (or small-scale) contamination, and diffuse contamination [17,26]; this approach deserves further development and broader use in environmental geochemistry.

This work aims to finally decipher the contribution of geogenic and anthropogenic components to elevated concentrations of PTEs in soils of the Ore Mountains. The region is a typical representative of geochemically complex areas with unknown anthropogenic contribution to severely elevated soil PTEs [2,14,15,18]. Although detailed geochemical soil mapping has been performed in the German part of the Ore Mountains by Saxon state authority LfULG [14], there is no overview of historical emission sources and their impacts on that area. This paper is focused on two particular areas in the Ore Mountains, Fláje and Kovářská, and demonstrates that dense sampling and EDA are indispensable to handling local soil complexity. The use of ECDFs for distinguishing diffuse contamination is a particular focus of this work, as some theoretical prerequisites used by Fabian et al. [17] need more attention in our study area; in particular, the diffuse contamination cannot be approximated by a perfectly homogeneous blanket over the entire impacted area due to local topographic and land cover variability (Figure 1). The strategic aim of this work is to test procedures of the separation of anthropogenic impact on soil PTEs applicable in whatever geogenically anomalous areas with long-term human impact on the entire environmental compartments, but fully respecting the real complexity of geochemical data mining. These tools could finally fill the gap of missing quantification of the historical emissions in the Ore Mountains.

2. Materials and Methods

2.1. Geography and Mining and Smelting History of the Study Area

The Ore Mountains (Erzgebirge in German and Krušné Hory in Czech) represent a mountain range stretching from SW to NE along the Czech-German state border (Figure 2). The altitude is between 338 and 1244 m a.s.l., and annual precipitation is about 900–1200 mm. Study areas are in the mountain ridge, from which the landscape gently slopes to the northwest. Although the Ore Mountains represented a natural barrier to landscape settlement in prehistoric times, their mineral resources made this area the most densely populated mountain range in mediaeval Europe [33–35]. The reasons for the colonisation of the Ore Mountains were glass and charcoal production and mining [36]. The mining activity, dating back to the Middle Ages, was primarily focused on Ag and Sn at the beginning; later Pb, Fe, Cu, Co, W, and U were also exploited [11]. Mining and metal smelting became dominant there in the 12th century and continued until the 20th century [11,12]. Mining significantly transformed the local landscape through deforestation and the establishment of settlements. Now the Ore Mountains are characterised by the abundance of old mining pits and spoil heaps, often close to the pastures and meadows.

The oldest rocks in the Ore Mountains are of Proterozoic and Cambrian-Ordovician age, exposed and transformed by regional metamorphosis, forming hard rocks similar to the younger granite massifs. The main rocks in the Ore Mountains are metamorphic rocks with predominant gneisses, quartzites, and amphibolites, as well as bodies of igneous rocks.

The Fláje Area (Figure 2) covers ca. 80 km^2. It is located around the former Fleyh village, now the Fláje Reservoir (1951–1964). The main rocks here are mainly granites and gneisses, formed from pelitic and granitic rocks; less abundant are amphibolites, basaltoids, and volcanic rocks. The area is rather exceptional for the Ore Mountains because of the absence of the past local mining and smelting. In the village of Moldava (Moldau) and its surroundings, glass was made in the 14th–17th centuries [37,38]. In Grünthal, ca. 15 km west of the Fláje Area (Figure 2), there were silver-copper liquation works for the separation

of Ag from "black copper" or "black lead" since the 16th century [34]. Other possible sources of emissions were in Mikulov and Hrob, ca. 5 km south-east of the Fláje Area, with the historical extraction of Ag-bearing polymetallic ores that peaked around the 16th century. More than 70 ore-bearing polymetallic veins of the As–Ag–Pb type have been documented in the zone between Hrob and Moldava. The mining complex also included a smelting furnace with amalgamation [39].

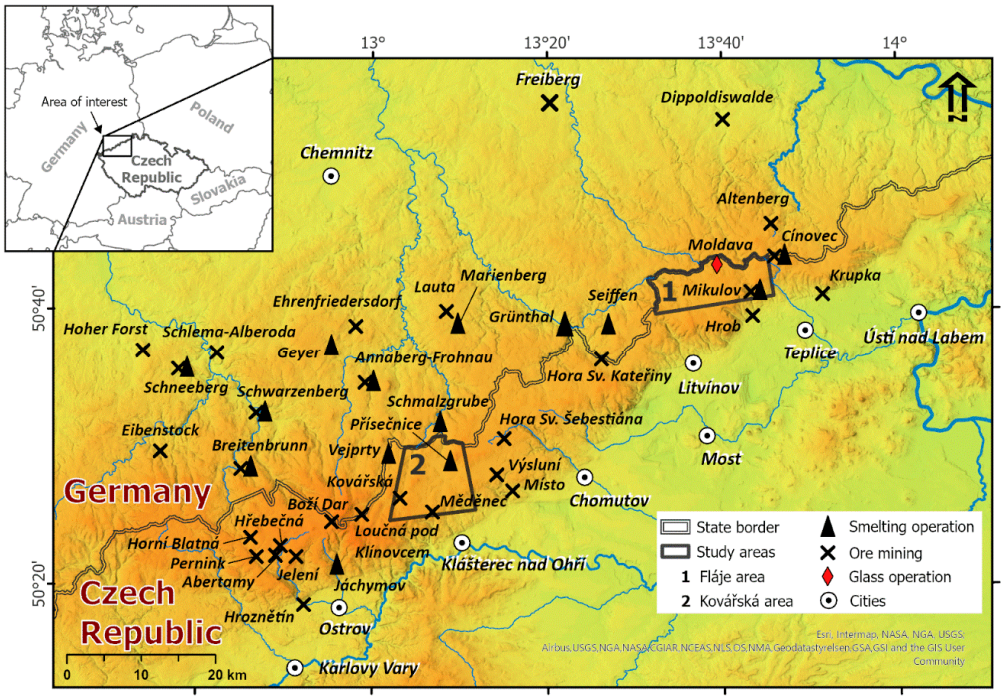


Figure 2. Overview map with marked study areas and with local evidence of mining, metallurgy, and glassworks.

The Kovářská Area is ca. 70 km^2 (Figure 2). Pelitic rocks to paragneiss are prevailing, with occasional surficial occurrences of basalts, metagranites, and peat. The whole area has mainly been affected by Fe mining and metallurgy since the 13th century. Polymetallic ores were mined and processed in Vejprty (Weipert), Měděnec (Kupferberg), and Přísečnice (Pressnitz), the last being the second most important Fe mining area in the Czech Lands until the end of the 19th century. The first blast furnace in Czechia was built in Kovářská (Schmiedeberg). Magnetite was the latest exploited ore, discovered at Měděnec in 1955 and mined from 1968 to 1992. Ironworks were also established in Schmalzgrube in Germany (Figure 2) in 1659; they were located ca. 6 km to the north of the Kovářská Area and produced pig iron [34].

2.2. Soil Sampling and Element Analysis

Soils were sampled after removing the O-horizon using a shovel or soil auger. The first sample (topsoil, TOP) was taken from a depth of 10 cm, which encompasses the A horizons. The second sample (deeper horizon, BOT) was from a depth of 40 cm; in shallow soils, the sampling depth for BOT was reduced to 30 cm. In each sampling, we collected about 200–300 g of soil. A total of 72 TOP and BOT pairs of soils were taken in the Kovářská Area and 101 pairs in the Fláje Area. Sampling was carried out at least 50 m away from main roads.

To post-stratify the samples into groups according to geology, we used the GeoCR online geological map with a resolution of 1:50,000 [40].

2.3. Element Analysis

The collected soils were air-dried at room temperature and sieved to a fraction $\leq$ 2 mm, pulverised in a planetary mill with zirconia vessel and balls (Pulverisette 6, Fritsch, Markt Einersheim, Germany), and homogenised and analysed for contents of PTEs (Cu, Pb, Zn) and lithogenic elements (Fe, Rb, Ti, Al) by table XRF spectrometer Epsilon 3X spectrometer (PANalytical, Almelo, The Netherlands) equipped with an X-ray tube (Ag cathode, up to 50 kV). Powdered samples were poured into conventional polyamide measuring cells with Mylar foil bottoms. The analytical signal was calibrated using certified reference materials IAEA SL-1, IAEA SL-3, and IAEA-314 Stream Sediment (IAEA, Wien, Austria), 2702 Inorganics in Marine Sediment, 1646a Estuarine Sediment, 2704 Buffalo River Sediment, 2710a Montana I Soil and 2711a Montana II Soil (NIST, Gaithersburg, MD, USA), CTA-FFA-1 Fine Fly Ash (Institute of Nuclear Chemistry and Technology, Warsaw, Poland), and BCR 176R and ERM-CC141 Loam Soil (Institute for Reference Materials and Measurements, Geel, Belgium) as described elsewhere [41]. Arsenic was determined using a handheld XRF spectrometer Niton XL3t 950 GOLDD + (Thermo Scientific, Waltham, MA, USA) with a 50 kV X-ray tube with a Ag cathode.

2.4. Geochemical Normalization

Mathematical properties of compositional data substantiate the use of element ratios rather than raw element concentrations in data processing [18,41,42]. The simplest and empirically justified way is to divide concentrations of a PTE (M) by the concentration of a suitable lithogenic element (M_{REF}), such as Al, Ti, Rb, Fe, Zr, or Y and thus use element ratios M/M_{REF} instead of M [43–46]. Geochemical normalisation corrects for the influence of the soil matrix [43], in particular, a variable percentage of soil organic matter (it is vital for the comparison of TOP and BOT, with more organic matter present in TOP) and quartz content (it is mostly controlled by the soil coarseness and this in turn by preceding particle segregation through slope processes and pedogenesis). Normalisation can transform geochemical datasets to be closer to normal (Gaussian) distribution [46] or at least to have a "sharper" main population of datasets, which considerably improves the identification of anomalous values [18,41]. We followed a similar approach for all the PTEs examined, also choosing Fe as a normaliser for Cu and Zn, as justified by Matys Grygar and Popelka [46]. In the Ore Mountain bedrock, As, Cu, Fe, and Zn usually occur jointly in sulphides (arsenopyrite, chalcopyrite) and dark minerals rich in Fe, such as biotites; all those listed elements also share the same pathways in weathering, pedogenesis, and possible soil transport by joint bonding to paedogenic iron oxides and other soil microparticles. Conversely, for Pb, Ti, a conservative element moderately abundant in several resistant volcanic mineral phases, has been empirically most useful as a normalising element, because those two elements show similar geochemical behaviour [47].

2.5. Empirical Cumulative Distribution Function

ECDF has traditionally been used to evaluate mono- or polymodality in data series and define outliers, particularly in ore prospection [28]. For similar purposes, ECDFs were later used in environmental geochemistry studies [17,18,48]. In addition, ECDFs are useful in data classification for the geochemical maps in a similar way to that used by Matys Grygar et al. [18].

Fabian et al. [17] proposed to utilise ECDF for the comparison of TOP and BOT concentrations and thus distinguish geogenic anomalies, diffuse and point source pollution, and surface enrichment by plan–soil interactions (Figure 1). The method by Fabian et al. [17] has further been employed by Reimann and Fabian [49] and Flem et al. [50] and is also used in this paper. To estimate diffuse contamination after Fabian et al. [17], we searched for an optimal horizontal shift of the BOT ECDF to get the best visually evaluated overlap with the TOP ECDF by choosing a suitable *a* in equation

$$M_{TOP} = a \cdot M_{BOT} + b, \quad (1)$$

where a represents linear shift constant (LCS) and b corresponds to diffuse contamination [17]. The parameters a and b were estimated graphically by horizontally shifting BOT in the diagram to optimally overlay TOP visually; this shift corresponds to the visually optimal LCS parameter a. Contrarily to Fabian et al. [17], who optimised b to get the best match in the lower percentiles, we optimised it by matching the values in the 2nd and 3rd quartiles (Q2 and Q3), as we preferred not to rely on low outliers in the data series.

The part of the TOP curve with a steeper gradient compared to the BOT curve was evaluated as a contribution to diffuse contamination. The median for each PTE was calculated from the difference of the TOP and BOT diagrams using Equation (1).

2.6. Software for Data Processing

The data series were analysed using Origin 2018 software (OriginLab 95E, Northampton, MA, USA). Boxplots and ECDFs were created using the same software. The concentrations of PTEs and their local emissions were graphically represented using maps with classified layers, created in ArcGIS 10.7.1 Desktop software (ESRI, Redlands, CA, USA).

3. Results

3.1. PTE Concentration in Soils

The concentrations of the selected elements in the studied soils (Table 1) varied significantly. Several criteria were used to understand the PTE variability in soils. Firstly, we compared the total element concentrations in all 270 samples with the global (composition of the upper continental crust, UCC [51]) and European background (FOREGS database, >1500 randomly selected mineral soil samples from 26 European countries, [52]) and the national averages (Figure 3 and Table 1). Arsenic and Pb exceed these backgrounds and national averages considerably, Cu is close to UCC and FOREGS at both sites, and Zn is elevated in the Kovářská Area (Figure 3).

Table 1. A summary of medians for individual PTEs and rock groups in mg kg^{-1}. In the last column of the table, UCC and FOREGS values in mg kg^{-1} are shown for comparison. The label "all rocks" means the median value for the whole area, without division into rock groups.

		Amphibolites	Basaltoids	Metagranitoids	Metapelites	Peat	Fluvial Sediments	Granitoids	Volcanic	All Rocks	FOREGS
Fláje Area	As TOP	418	63	104	72	46	x	34	54	62	7
	As BOT	134	62	92	54	16	x	27	47	52	6
	Cu TOP	27	19	20	23	36	x	17	13	20	13
	Cu BOT	25	19	16	23	24	x	16	10	19	14
	Pb TOP	157	168	173	165	218	x	110	155	141	23
	Pb BOT	113	126	117	112	109	x	84	119	109	17
	Zn TOP	84	98	72	98	81	x	61	53	72	52
	Zn BOT	83	97	65	90	83	x	66	47	77	47
											UCC
Kovářská Area	As TOP	74	101	43	59	58	57	x	x	58	4.8
	As BOT	47	89	19	40	36	28	x	x	36	
	Cu TOP	28	28	12	26	29	25	x	x	25	28
	Cu BOT	30	23	11	23	25	16	x	x	22	
	Pb TOP	114	205	94	94	135	100	x	x	96	17
	Pb BOT	64	155	51	52	47	47	x	x	52	
	Zn TOP	174	170	43	130	73	137	x	x	116	67
	Zn BOT	207	152	49	105	67	93	x	x	98	

In addition, As and Pb concentration in both areas exceeds Czech legislative limits for agricultural soils according to Decree No. 153/2016 Coll. [53], while Cu and Zn do not exceed this limit. Soils from the Fláje Area have similar median As concentrations in TOP and BOT as the Kovářská Area (see Figure 3). The situation is similar for Cu, and the

median values are also similar in the areas, although the highest values are considerably higher in the Kovářská Area. Lead concentrations are thus clearly higher in the Fláje Area, including the extremely high values in TOP and BOT. In contrast, Zn concentrations are higher in the Kovářská Area (see Table 1).

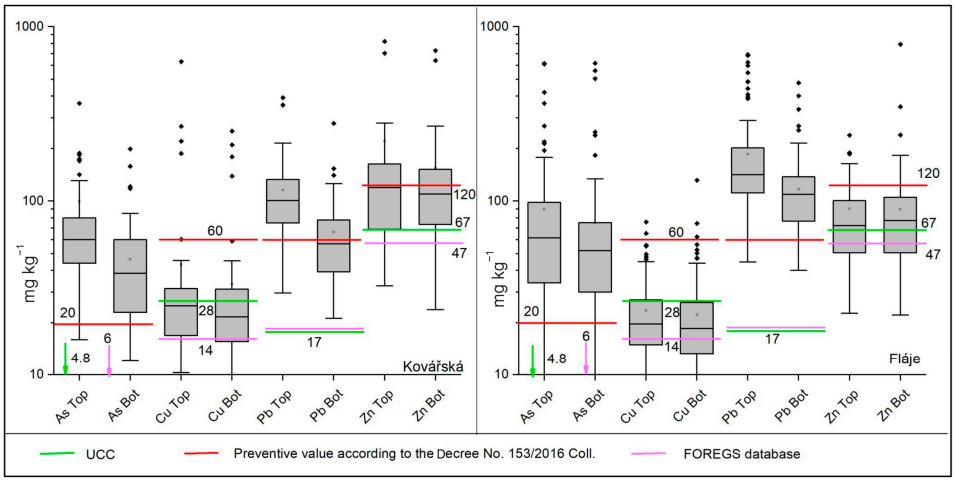


Figure 3. The summary of raw (non-normalised) concentrations of PTEs (mg kg^{-1}) for the two study areas with highlighted selected reference values.

The separation of samples into groups according to bedrock geology showed that the geogenic influence on soil PTEs is not equal at both study sites. A more pronounced impact of geology was found in the Fláje Area (Figures 4 and 5), where the concentrations of PTEs expressed as Cu/Fe, Pb/Ti, and Zn/Fe in the TOP and BOT samples are lower in soils formed from basalts and amphibolites and higher in the peat soils. High values are observed for As/Fe in the soils on amphibolites, and highly variable topsoils As/Fe and Cu/Fe were found on granitoids.

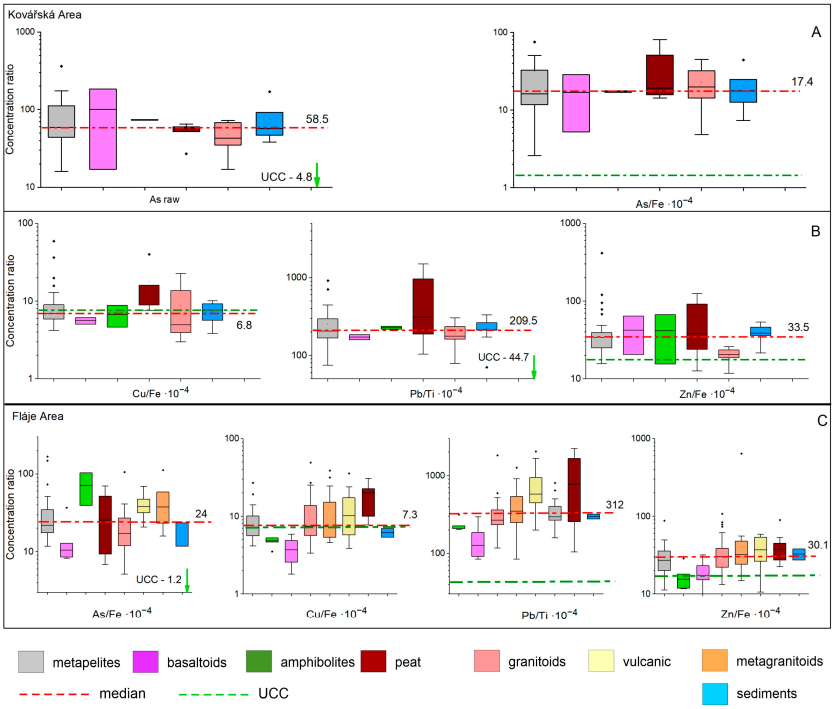


Figure 4. Concentrations of PTEs in TOP (10 cm) divided by bedrock and areas with medians (red line) and UCCs (green line or arrow) indicated. Example of raw data vs. normalisation (**A**) and normalised PTEs of the Kovářská Area (**B**). (**C**) Normalised PTEs of the Fláje Area.

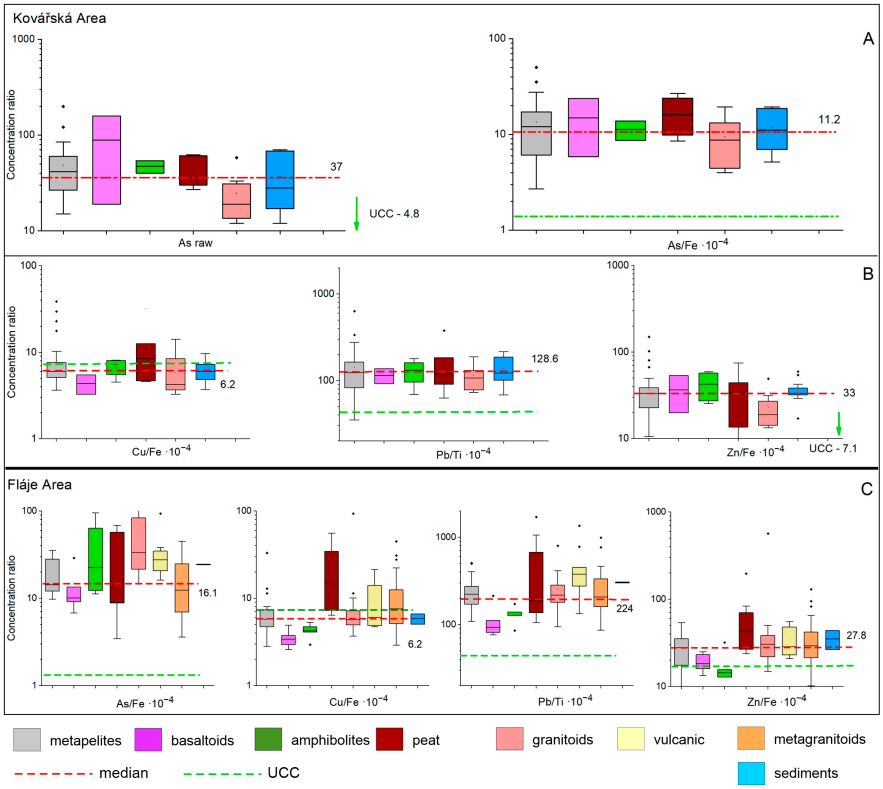


Figure 5. Concentrations of PTEs in BOT (40 cm) divided by bedrock and sites with medians (red line) and UCCs (green line or arrow) indicated. Example of raw data vs. normalisation (**A**) and normalised PTEs of the Kovářská Area (**B**). (**C**) Normalised PTEs of the Fláje Area.

At the Kovářská Area, there is no significant group of rocks with exceptionally high concentrations of normalised PTEs compared to other groups. Figure 4 (TOP) and Figure 5 (BOT) show, how Fe normalisation helps to mitigate the effect of soil textural variability on As concentrations, allowing all rock groups to be worked with in a single plot, or to approximate the medians of each group to each other, including peat, which remains anomalous compared to the other rock groups. Overall, TOP is enriched compared to BOT for As/Fe and Pb/Ti in both study areas. Contrarily, the median Cu/Fe and Zn/Fe concentrations in TOP and BOT are quite similar and close to the UCC at both sites. Figures 4 and 5 show, how Fe normalisation of As concentrations helped to mitigate the effect of the bedrock variability on soil composition, allowing all rock groups to be worked with in a single plot, or to approximate the medians of each group to each other, including peat. This data treatment was effective and was thus used for all studied elements.

3.2. Geochemical Maps

To examine the spatial distribution of PTEs, we constructed a geochemical map with TOP and BOT composition using classified layers. Four individual concentration classes were defined by ECDF (Figures 6 and 7; for details of the classification, see Figure 6C) for the geochemical maps (Figures 8 and 9), where green and yellow colours indicate background or moderate contamination, orange is defined as moderate contamination, and red indicates anomalous values and severe contamination.

In the Kovářská Area, the high values of PTE are most abundant near Mědník Hill (Figure 8). This is particularly evident for Cu/Fe and Zn/Fe, their concentration ratios decreasing with distance from this mining site. However, another mechanism has controlled As/Fe and Pb/Ti, as their high TOP values are scattered over the entire area, with no apparent decrease with distance from the mining site, but rather forming a belt to the north of the Mědník Hill.

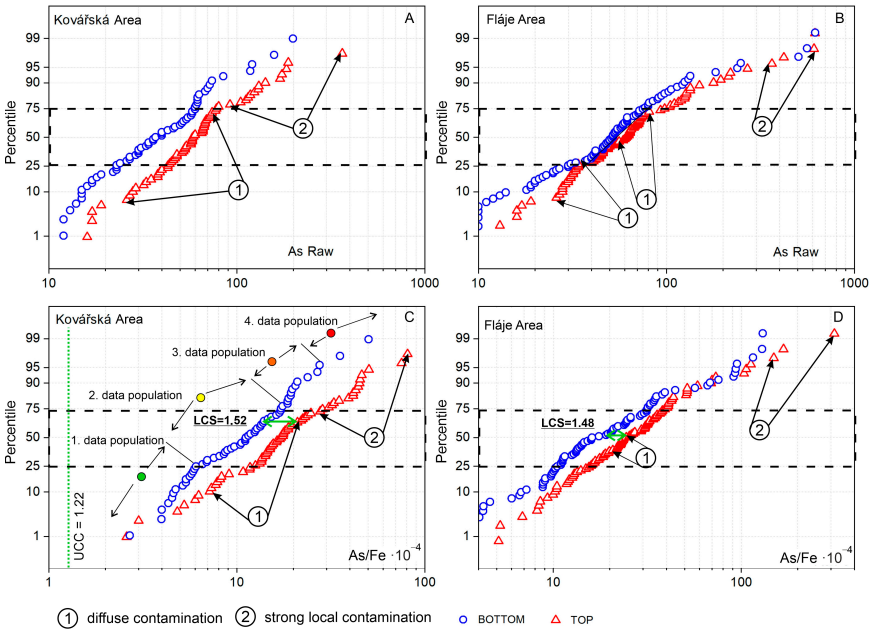


Figure 6. Comparison of raw (**A**,**B**) and Fe-normalised As concentrations (**C**,**D**) in soils using ECDF plots, divided into TOP and BOT. Part 6C shows the classification of data by natural breaks to data populations. Parts of probable diffuse and severe point contamination are marked by arrows. The green line indicates the UCC value.

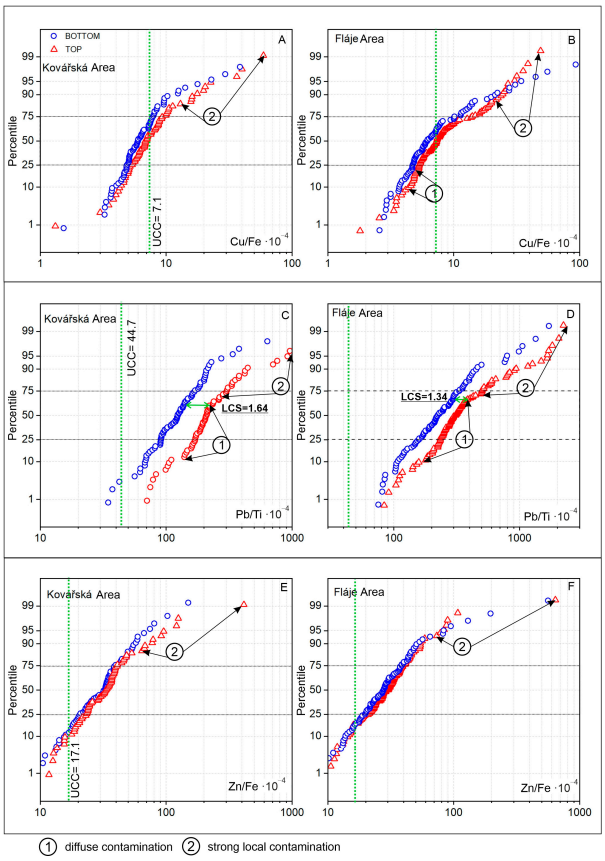


Figure 7. Ti and Fe-normalised concentrations of Cu/Fe (**A**,**B**), Pb/Ti (**C**,**D**) and Zn/Fe (**E**,**F**) in soils using ECDF plots, divided into TOP and BOT. Probable diffuse and severe point contamination are marked by arrows. The green line indicates the UCC value.

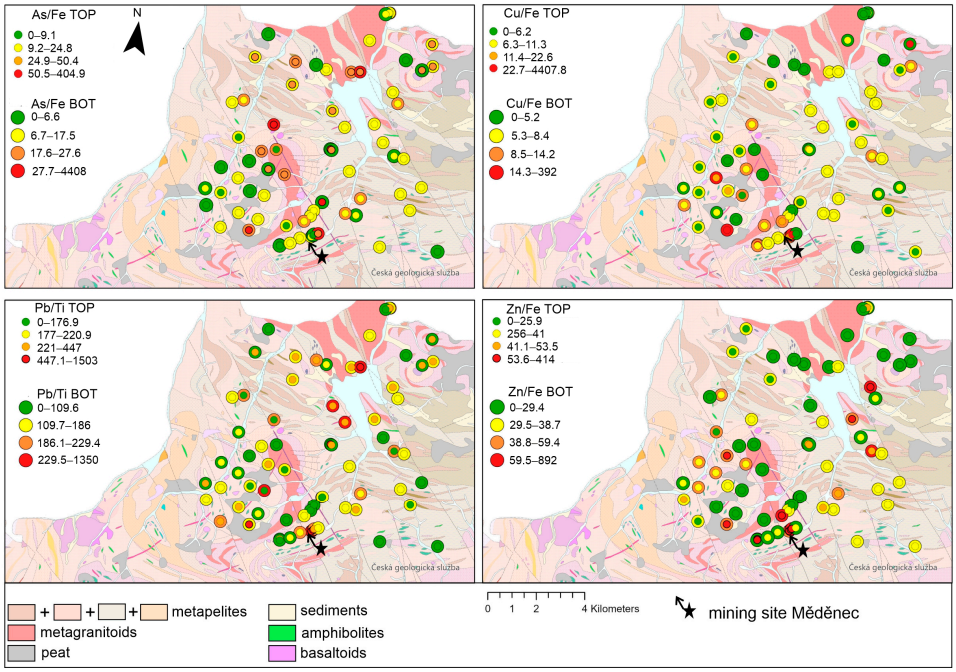


Figure 8. Geochemical map with TOP and BOT distribution in concentration ratio, Kovářská Area.

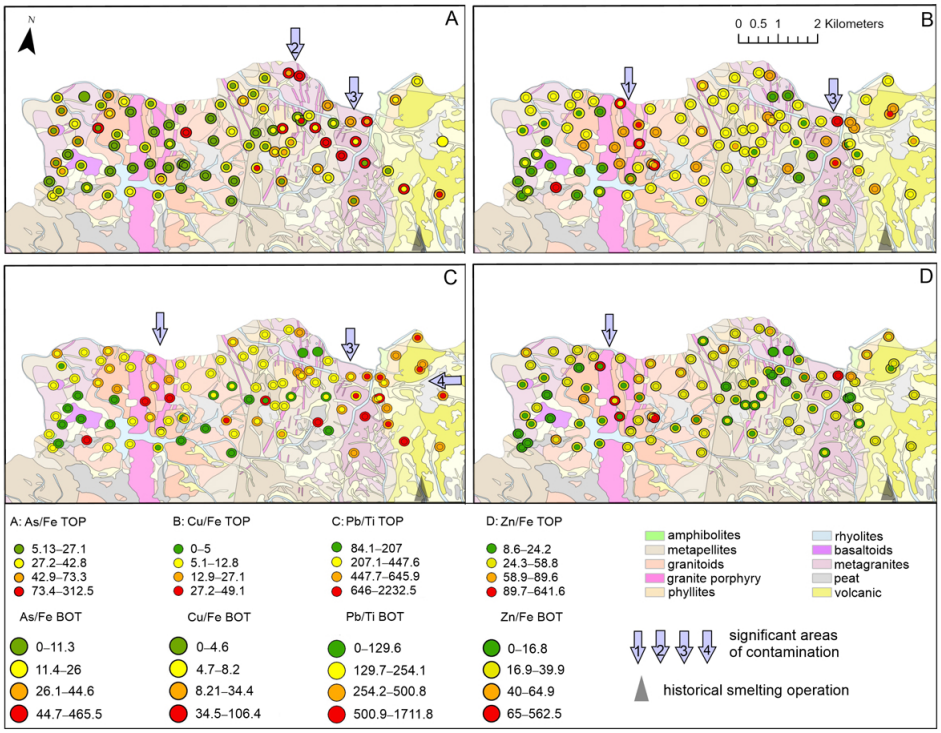


Figure 9. Geochemical map with TOP and BOT distribution in concentration ratios—the Fláje Area.

In the Fláje Area (Figure 9), several sites were found to be distinctive. The first (arrow 1 in Figure 9) is around the locally prominent granitic porphyry outcrop at the Fláje Reservoir with several spots with elevated Pb/Ti, Cu/Fe, and Zn/Fe in the TOP and BOT, indicating the influence of the underlying rocks, possibly with local ore veins. The second area (arrow 2 in Figure 9) is primarily significant for As/Fe and is close to local historic glassworks in Moldava. Several other soils classified as severely contaminated (high As/Fe, Cu/Fe, and in particular Pb/Ti) are found on the eastern side of the area (arrows 3 and 4 in Figure 9). These spots cannot be attributed to bedrock geology alone, as only topsoils are

contaminated. However, these soils are close to local mining sites and a smelting furnace near the Hrob mining and smelting site (see Figure 2).

3.3. Comparison of PTE Concentrations in TOP and BOT Using ECDF

ECDFs of TOP and BOT (Figures 6 and 7) show the TOP enrichment for As/Fe and especially Pb/Ti at both sites and in contrast, none or weak TOP enrichment for Cu/Fe and Zn/Fe, except for individual point-contaminated samples near spoil heaps (Figure 8, points near the Mědník Hill). ECDFs make it possible to examine the effect of geochemical normalisation of PTE concentrations, as demonstrated by the example of raw As (Figure 6A,B) and As/Fe (Figure 6C,D). Geochemical normalisation turns the more heterogeneous/polymodal ECDF of the raw As data series to a clearer and smoother ECDF of the As/Fe element ratio. This is more evident in the geologically more complex Fláje Area (Figure 6B—before normalisation) than in the Kovářská Area (Figure 6A), and the effect of normalisation is clearer in Figure 6D. ECDFs show how the influences of the soil matrix and bedrock impact are corrected and the dataset and made more readable through geochemical normalisation, which is demonstrated in Figures 4A and 5A, where this effect is also visible.

ECDF offers an alternative to examine the interrelation between TOP and BOT in maps with classified layers focused on their spatial distribution (Figures 8 and 9) and boxplots producing net overall TOP contamination (Figure 4). The ECDF alternative proposed by Fabian et al. [17] is specified in Section 2.5. When evaluating the total As/Fe concentration ratio, it is evident that the linear shift of TOP by the choice of a (Equation (1)) is slightly larger in the Kovářská Area (Figure 6C), so there are probably more controlling factors in that area. The As/Fe concentration ratios in Q2 and Q3 in the Kovářská Area range from 6.5×10^{-4} to 17×10^{-4} for BOT and from 13×10^{-4} to 28×10^{-4} for TOP. There are also several high outliers in the As/Fe data series (roughly above the 75th percentile), likely because of severe local contamination from mining in Měděnec. Those high outliers form a bulge at high values separated from Q3 by a break in the ECDF curve (Figure 6C). Thus, about 25% of the samples (entire Q4) in the area have been locally anthropogenically contaminated. In the Fláje Area, the values for As/Fe in Q2 + Q3 are 10×10^{-4} to 31×10^{-4} concentration ratios for BOT and 16×10^{-4} to 39×10^{-4} concentration ratios for TOP. There are only a few high anomalies in the Fláje Area, where the overall elevated soil PTE concentrations result mainly from the combination of geogenic causes and diffuse contamination.

TOPs are little enriched relative to BOT for Cu/Fe and Zn/Fe (Figure 7A,B,E,F); in the case of Zn TOP and BOT, the ECDFs almost overlap even without adjustments according to Equation (1). However, there are a few outliers at both sites. In the Kovářská Area, this is evident for both Cu/Fe and Zn/Fe at about the 80th percentile, where the bulge is, and this can correspond to the mining sites around the top of Mědník Hill, as shown in Figure 7A,E. In the Fláje Area, the high Zn/Fe ratio around the 95th percentile is probably related to the geogenic source, granitic porphyry, as it is obvious from the spatial association of the high TOP and BOT values (Figure 9, arrow 1). Overall, there is no significant Cu/Fe and Zn/Fe emission enrichment in TOP.

In contrast, Pb appears to be the main emission (surficial) soil contaminant in both areas (Figure 8). The median Pb/Ti concentration ratios in the BOT layer are significantly higher in the Fláje Area (224×10^{-4}) than in the Kovářská Area (130×10^{-4}), which indicates naturally higher Pb concentrations already in the soil parent rocks. From about the 75th percentile onwards, a significant bulge deviates from the subsoil curve. This is characteristic of a severe local contamination source or the combined influence of mineralisation and local anthropogenic contamination.

The Kovářská area shows higher Pb/Ti TOP enrichment and a more significant linear shift (Figure 7C). However, the concentration ratios in the preferentially studied Q2 and Q3 are lower here: TOP (170–300) $\times 10^{-4}$; BOT (90–170) $\times 10^{-4}$ compared to the TOP (230–500) $\times 10^{-4}$; BOT (160–320) $\times 10^{-4}$ in the Fláje Area (Figure 7D). The TOP curve again shows a bulge of high outliers starting at approximately the 75th percentile. The

enrichment of topsoil in As/Fe and Pb/Ti and the steeper gradient between the TOP and BOT diagrams further suggest that both areas have been affected to some extent by diffuse contamination (marked in Figures 6 and 7).

3.4. Quantification of Diffuse Contamination using ECDF of Entire Data Series

For the application of Equation (1), we focused mainly on Q2 and Q3, in which we looked for signs of diffuse contamination and then calculated its contribution to the total contamination with As/Fe in the Kovářská Area and Pb/Ti in both areas. The results are presented in Table 2. Because the LCS is a statistical average for the entire BOT and TOP data series, it neither reflects every single point nor represents true pairs of TOP and BOT for each sampling site. LCS thus only provide bulk and coarse estimates assuming a perfectly homogeneous blanket of diffuse contamination.

Table 2. Summary of LCS (*a* in Equation (1)) and predicted diffuse contamination concentration ratios for each element and area.

	Kovářská			**Fláje**	
	LCS	**Estimated Diffuse Contamination**		**LCS**	**Estimated Diffuse Contamination**
As/Fe	1.52	1.12	As/Fe	1.48	1.42
Pb/Ti	1.64	16.5	Pb/Ti	1.34	16.2

For the Kovářská Area, diffuse contamination is not surprising given the abundance of local contamination sources (Figure 2) and it reaches 16.5×10^{-4} for Pb/Ti and 1.1×10^{-4} As/Fe (concentration ratios) for Q2 and Q3. However, for the Fláje Area, where we did not expect contamination because of no local mines or furnaces being in existence, the calculations produced results very similar to those in the Kovářská Area (see Table 2). We estimated the linear concentration shift as 1.48 for As/Fe and the diffuse contamination contribution as 1.42 concentration ratio for Q2 and Q3. For Pb/Ti, with the diffusion contribution as high as 16.2×10^{-4} concentration ratio and the LCS at 1.34. This suggests that there has been a significant emission source outside the Fláje Area (Figure 9), i.e., more remote, and perhaps common for both study areas.

3.5. Quantification of Diffuse Contamination Using TOP and BOT Pairs

The method to evaluate TOP and BOT differences in a rough, but in a sense more straightforward manner than using Equation (1), is a graphical presentation of TOP and BOT differences in a geochemical map, classified based on ECDF diagrams (Figure 10). In contrast to the approach based on Equation (1), these maps show a real paired comparison of TOP and BOT for each sampling point (Figures 11 and 12), while in the ECDFs approach by Fabian et al. [17] the TOP and BOT pairs are disconnected. The TOP–BOT approach keeps the pairs connected but works with raw concentrations, which is not mathematically correct (see Section 2.4); however, it produces direct estimates of TOP enrichment in concentration units. To express these estimates for the whole area, the medians for each element are presented in Table 3. The plain TOP–BOT difference in the ECDF plot in Figure 10 shows the distribution of the values around zero, consistently with a lack of net diffuse contamination of TOP for those two elements. This situation is common in the Kovářská Area near mining sites at Mědník Hill (Figure 8).

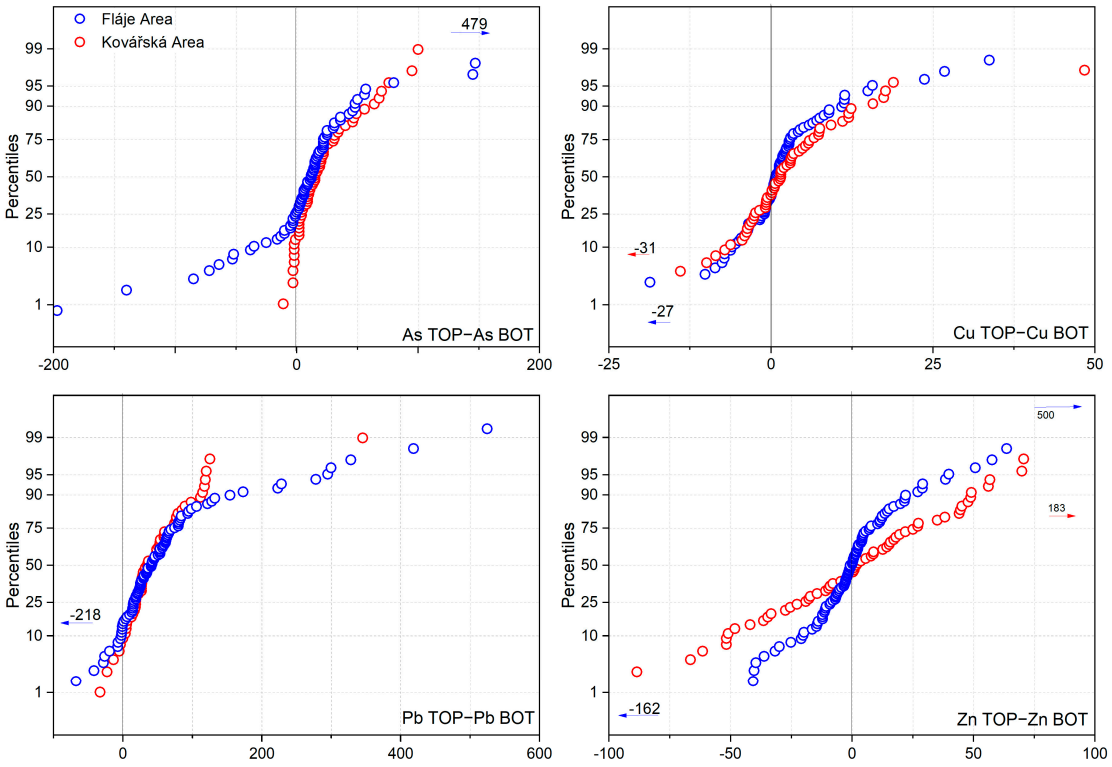


Figure 10. A representation of the emission contribution (mg kg^{-1}) of individual PTEs using the TOP minus BOT methodology.

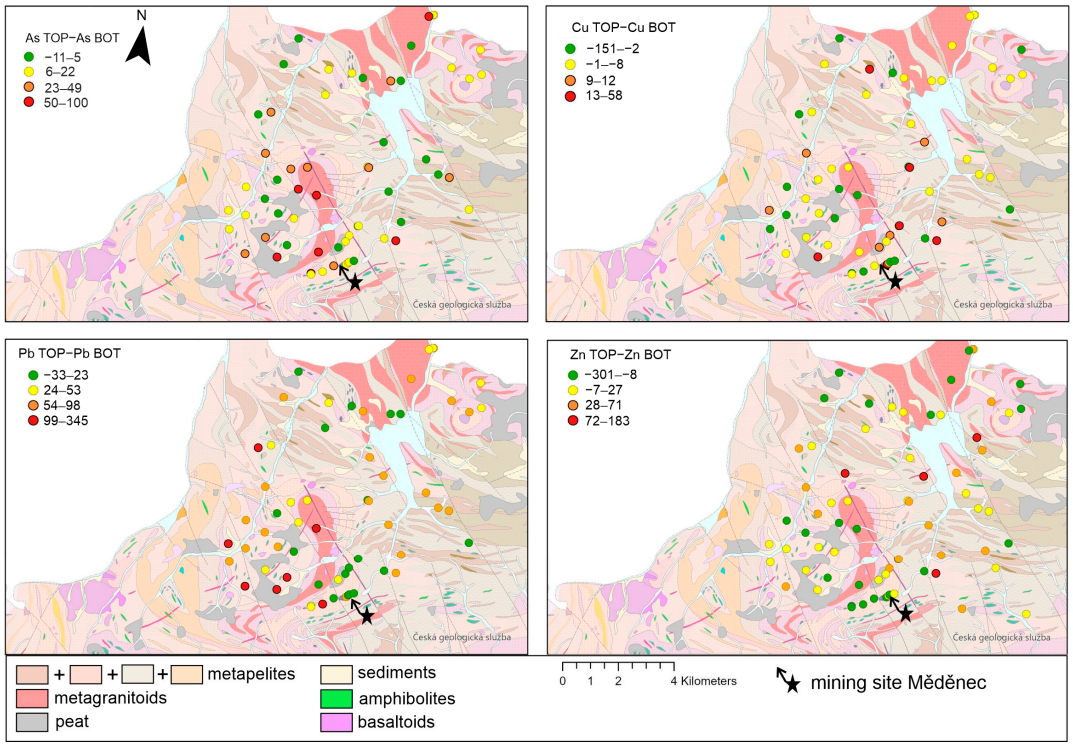


Figure 11. An overview map of the Kovářská Area and plotted TOP–BOT values (mg kg^{-1}), expressing the net contribution (emissions) of individual PTEs.

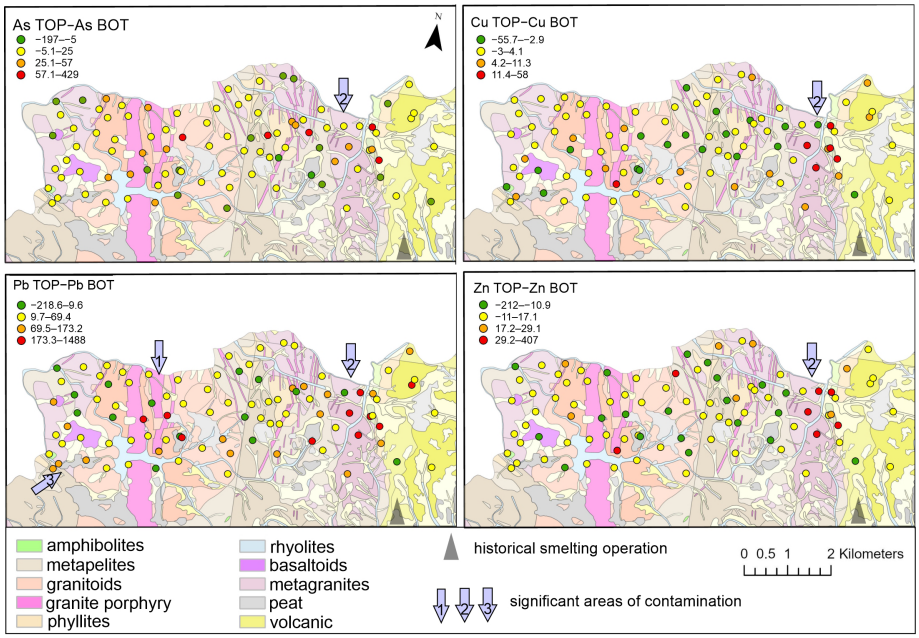


Figure 12. An overview map of the Fláje Area and plotted TOP–BOT values (mg kg^{-1}), expressing the net TOP contribution (emission enrichment) of individual PTEs.

Table 3. Summary of medians for TOP–BOT difference in mg kg^{-1}.

Element	Kovářská Area	Fláje Area
As	15	14
Cu	1.5	0.7
Pb	35	42
Zn	1.7	−0.7

Figure 13 compares TOP/BOT enrichment factors for each of the examined PTEs in its geochemically normalised form to compare relative surface enrichment by emission contamination. Also, TOP/BOT evaluation shows the topsoil enrichment decreases in the order Pb/Ti > As/Fe > Cu/Fe > Zn/Fe for both areas, except for two high Cu/Fe outliers in the Fláje Area.

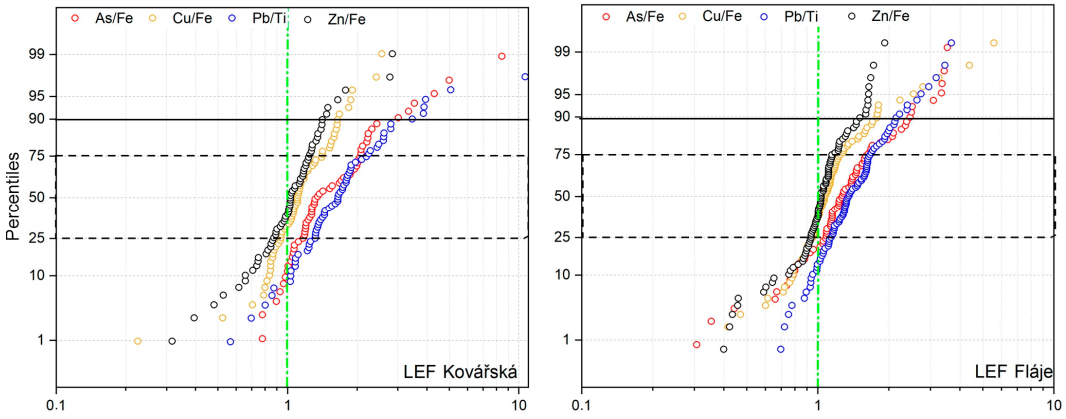


Figure 13. Local enrichment factors (LEF) expressing the difference in concentrations (mg kg^{-1}) of PTEs in TOP versus BOT. The green line represents the LEF=1 threshold representing an unpolluted to slightly enriched TOP layer.

4. Discussion

4.1. Impact of Soil-Forming Substrate on PTE Concentrations

It is generally accepted in the assessment of soil contamination that the parent rock is one of the most important RCFs for PTEs in soils. It can be revealed in the spatial display of the data obtained on a map with the geology of the area or the post-stratification (separation) of concentration data into groups according to geology (Figures 4 and 5). The influence of geology on the concentrations of PTEs has been addressed in several papers [8,11], with the result that certain groups such as ultramafic, mafic, and granitic rocks are so prominent that they need to be considered separately when evaluating the soil composition datasets. The influence of geology as one of the fundamental RCFs is also evident in this study, although less significantly than we initially expected. Unless contrasting geology, such as basalts and granitoids, is involved, geological variability seems less significant on such a small scale than when mapped on a national scale, as shown by [19].

Geology plays a significant role in the Ore Mountains for As and Pb (As/Fe and Pb/Ti), but not in the sense of variability among individual geological units, but rather as an overall enrichment of PTEs in soils of the Ore Mountains compared to global (UCC) or regional (FOREGS) surveys, which seems to be related to metamorphosis and associated formation of ore veins. Comparisons of local PTE concentrations with the global or European backgrounds must take local specificity into account because natural PTE concentrations in soils can vary significantly from area to area, within and between regions, making it impossible to define single global background values [54]. Peat and organic matter in general appeared as the most anomalous soil-forming substrates in our study, a parameter that needs to be addressed frequently in temperate mountain areas. The elevated PTEs volatilised by ore roasting and metallurgy (As and Pb), scavenged by plants and then transformed to peat (Figures 4 and 5) attest to emissions in the area; this is due to the sorption capacity of organic matter, which acts as a geochemical trap [16]. Conversely, Cu and Zn are sorbed on soil Fe oxides rather than on organic matter and thus elevated organic matter in TOP mainly dilutes their concentrations in soils, which is corrected with geochemical normalisation (Figures 4 and 5), also efficient in weakening soil matrix effects.

O'Shea [55] described elevated As concentrations in metasedimentary rocks, up to 138 mg kg^{-1}, of which one possible cause is the impact of large-scale fluid flux during rock metamorphosis [56]. Among these rocks, marine pelitic protoliths (such as the gneisses in the Ore Mountains, see Figure 5) typically show the highest average As concentrations ($\sim$18 mg kg^{-1}). All parent rocks from the Ore Mountains are enriched in As. Arsenic concentration is most variable in basaltoids and metamorphosed rocks. In terms of rock types, Pb concentrations are frequently elevated in granite, followed by schist, gneiss, intermediate rocks, basic rocks, and ultramafic rocks [57]. Lead is widely dispersed in trace amounts in several common minerals, including K-feldspar, plagioclase, mica, zircon, and magnetite [52]. However, our results indicate that mineralization enrichment with Pb occurred throughout the entire area irrespective of the bedrock type.

The local background concentration ratios for As/Fe and Pb/Ti (7×10^{-4} and 95×10^{-4} in the Kovářská Area and 12×10^{-4} and 120×10^{-4} in the Fláje Area, respectively) are elevated relative reference values (Figures 6 and 7).

4.2. Use of ECDF and Geochemical Maps for Distinguishing Diffuse and Point Contamination

In geochemical mapping, the most challenging issue is how to correctly and objectively classify the data populations into background and contamination classes and how to define a threshold separating high outliers. The background population can be defined as the portion of values with the natural PTE content in soils without human influence [58]. For the actual classification of the data, ECDF diagrams are useful to show discontinuities (gaps) between the main concentration modes [59], including gaps separating anomalous values, as shown in Figure 6C. The contamination is then easily detectable in the upper part of the data series, e.g., in Q4 where the TOP "deviates" from the BOT and forms bulges (Figure 7C,D). However, the location of these bulges is not only linked to Q4; it depends on

the level of contamination and can generally also be found in the lower quartiles. Provided that such a classified dataset is displayed in conjunction with a geological map, there is a good chance of revealing any spatial links to rocks or contamination sources.

A considerable portion of soil samples from the Fláje Area with locally elevated Pb contamination originated from peat (Figure 9C). It reflects both emission scavenging by vegetation and the Pb-sorption capacity of organic matter, which acts as a geochemical trap for several elements [16].

A cluster of elevated As/Fe values is found in the east of the area (Figure 9A, arrows 2 and 3). This clustering is not associated with anomalous geology, but it is close to the local mining and smelting around cities Mikulov and Hrob [39] and glassworks around Moldava city (Figure 1). Another portion of the studied soils, mostly TOP classified as intermediate contamination (tagged by orange circles in Figure 9A), is distributed over a broad area and points to overall diffuse contamination of the entire area. Several TOP and BOT pairs (Cu/Fe, Pb/Ti, Zn/Fe) in the severely contaminated category (red colour in the map) occur in the western part of the Fláje Area (Figure 9B,D, arrow 1). Contamination at both depths can indicate a geogenic anomaly; most of these points are on granite and granitic porphyry geology, i.e., on metamorphosed rocks. However, the geology can play a role here as a secondary parameter and through the soil texture.

The Kovářská Area (Figure 8) is relatively simpler in terms of distinguishing anthropogenic contamination from geogenic anomalies. Strong local contamination is only evident around Mědník Hill, which dominates as a local source of all studied PTEs. The role of diffusive contamination of As/Fe and especially Pb/Ti is obvious around Kovářská.

4.3. Realistic Estimates of Diffuse Contamination Contribution

Contamination is commonly defined as the presence of unusually high concentrations in the data series, and soil contamination monitoring is usually focused on them. However, depending on the signal strength, local (point) contamination becomes indistinguishable from natural background variations in meters to several kilometres from the source [26]. Arsenic and lead are common diffuse contaminants due to their volatility in elemental (Pb) or oxidic forms (As_2O_3), particularly in areas like the Ore Mountains, with widespread sulphide ore roasting and silver production using ancient lead technologies, especially liquation (Section 2.1). The estimation of the diffuse input in this work is based on the assumption that Pb of anthropogenic origin is retained on the soil surface and the deep soil layers (BOT) originate mainly from the bedrock. Based on this assumption, Fabian et al. [17] proposed comparing the ECDFs of a PTE for TOP and BOT to identify and quantify diffuse contamination. This idea, further employed in subsequent works [29,30,50] is a powerful tool to overcome the problem of weak contamination, otherwise poorly distinguished by conventional data mining.

The idea by Fabian et al. [17], however, includes a model of a fairly homogenous spatial distribution of PTE emissions, which is not very likely in a real landscape, even over a small area, such as the study areas in the Ore Mountains as depicted schematically in Figure 1. The diffuse contamination of topsoils has been affected by variability in the past vegetation cover and its emission-scavenging performance, which is markedly different for meadows and forests. Additional heterogeneity inevitably resulted from varied topography and slope orientation relative to the emission sources and the preferential wind directions in the area. In TOP and BOT contamination following the ECDF approach by Fabian et al. [17], a challenge particularly relevant for the Ore Mountains is a difference of organic matter in topsoil content and generally different soil texture in TOP and BOT. To correct PTE concentrations for those factors, geochemical normalisation is used [44,46]. The geochemical normalisation can also "sharpen" the major concentration populations in geochemical datasets and thus improve their interpretability, in particular the definition of outliers [41,59]. Elements are also exchanged between TOP and BOT layers, either by biochemical processes in the form of a "plant pump", especially for elements such as Cd,

Zn, and Cu [16,60] (Figure 1). However, this plant pump is not quite so relevant for Pb and As, because as non-essential elements they are not involved directly in biotic cycling.

From a purely mathematical perspective, Fabian et al. [17] and his followers [29–31] assumed that the impact of the diffuse contamination is easiest and most sensitively distinguished in the low-end of the data series in ECDFs because the contamination input is most substantial there. The problem is that the lowest percentiles are found in soils with a high percentage of quartz sand and/or organic matter, where there is also the highest risk of post-depositional migration of contaminants; the consequent downward migration of emissions would lead to underestimation of the diffuse contamination contribution according to Equation (1). The lowest quartile or lower percentiles can also suffer from noise and bias analytical uncertainty. In our work, we preferred to search for diffuse contamination in the ECDF with special attention to Q2 and Q3.

The ECDF examination following methodology by Fabian et al. [17] is shown in Figures 6 and 7 and it confirms the results from the geochemical map (Figures 8 and 9): both study areas are affected by TOP diffuse enrichment of Cu/Fe contamination minimally, Zn/Fe barely, and As/Fe and Pb/Ti significantly. The TOP increase by diffuse contamination is somehow larger in the Fláje Area for As/Fe and Pb/Ti, although more local mining and smelting activities have occurred in the Kovářská Area. Following Fabian et al. [17], we calculated the diffusion contributions in both areas for Pb/Ti (16.5×10^{-4} for the Kovářská Area and 16.2×10^{-4} for the Fláje Area) and As/Fe (1.12×10^{-4} and 1.48×10^{-4}, respectively). Upon comparing the diffuse contamination components with the local background levels for As/Fe (7×10^{-4} and 12×10^{-4}) and Pb/Ti (95×10^{-4} and 120×10^{-4}, respectively), it appears that the emission contamination accounts for approximately 16% and 17% of the overall concentration in the Kovářská Area. Similarly, in the Fláje Area, these values are approximately 12% and 14%, respectively.

4.4. Diffuse Contribution from Soils and Peats and Outlines of Future Work

The most common way of evaluating the TOP and BOT contaminant concentrations is their division into enrichment (EF) or concentration factors (CF). The TOP/BOT ratio higher than 1 is conventionally attributed to anthropogenic pollution [61]. Such a ratio can then also be used to summarise the enrichment of topsoil for each element in a given area (Figure 13) to show which contaminants are relatively most important.

Fabian et al. [17] have made a major contribution by distinguishing relative TOP enrichment similar to EF or CF (this is the slope *a* in Equation (1)) and additive enrichment (intercept *b* in Equation (1)) and attributing the latter to diffuse contamination. The example of b evaluation is shown in Figure 10. The plain difference of raw concentrations in Figure 10 is a coarse approximation, which neglects the textural difference of TOP and BOT discussed above, but it provides a direct estimate of the net enrichment of TOP versus BOT by diffuse contamination and thus enables to compare results obtained by soil mapping with evaluation of the peat record. Bohdálková et al. [12] studied anthropogenic accumulations of Pb, As, and Cu in the peat core sampled near Kovářská village; they found emission fluxes ~6, 0.9, and 0.2 mg m^{-2} $year^{-1}$, respectively, in the period between years 1420 and 1650. The total Pb fallout for the time period 1500–2000 CE was estimated from the emission fluxes by Bohdálková et al. [12] to be 1.9 g m^{-2}, As fallout 0.35 g m^{-2}, and Cu fallout 0.2 g m^{-2}. Soil analyses, which we performed in the Kovářská Area, do not provide the temporal constraints for the emission flux, but they provide an estimate of total cumulative fallout soil contamination. In the Kovářská Area, the median Pb and As emissions (TOP–BOT differences) are 35 mg kg^{-1} and 15 mg kg^{-1}, respectively (Figure 10, Table 3). In the Fláje Area, the median of emissions for Pb is as high as 41 mg kg^{-1}, and 14 mg kg^{-1} for As, which is comparable to the Kovářská Area. Making rough assumptions on (i) the soil density of approximately 1.5 t m^{-3} [62], and (ii) all emissions having been captured in TOP, while (iii) BOT represents pre-anthropogenic background, the total fallout for Pb and As was 6 g m^{-2} and 2 g m^{-2}, respectively, for the Fláje Area, and 5 g m^{-2} and 2 g m^{-2}, respectively, for the Kovářská Area. Such estimates are only slightly higher

than those obtained from the peat archive by Bohdálková et al. [12]. A recent study by Shotyk et al. [63] indeed showed the peat archives could not "catch" and hold the entire emission fallout, and the co-incidence of our estimates and Bohdálková et al. [12] can thus be accepted. In contrast, results by Veron et al. [64], who analysed peat core near Boží Dar, not far south-west of Kovářská (Figure 1), declared more than an order of magnitude bigger total Pb emission fluxes lasting longer than it had been documented by archaeological and botanical research [12,36]; it would produce diffuse enrichment of local topsoils to several hundred ppm Pb that has not been found yet in the target area.

According to the emission fallouts and results of the spatial distribution of Pb and As TOP enrichment (Figures 11 and 12), the main sources of pollution are located outside the Fláje Area with rather small-scale mining and smelting activities south of the south-east corner of the Fláje Area (Figure 2). It is worth noting that prevailing wind directions in the Ore Mountains ridge are from the north-west to the east [65], which further weakens possible local contamination in the Fláje Area. Similarly, in the Kovářská Area, the impact of local metallurgy centres does not seem greatly relevant relative to overall TOP enrichment. Our findings thus indicate that the sources of diffuse contamination in the Czech part of the Ore Mountains ridge were located in Germany, likely in Grünthal, or even farther from here in Freiberg, which was the most important Ag mining and smelting centre in the Ore Mountains for several centuries (see Section 2.1). This surprising finding will surely motivate our further investigation, as it pinpoints the lack of knowledge on the past emission sources in the Ore Mountains. Yet only an overview of mining centres is available [35], which definitely not all produced As and Pb emissions.

5. Conclusions

Appropriate sampling and analytical strategy are indispensable for distinguishing geogenic anomalies from anthropogenic activity in mineralised and anthropogenised landscapes, including top and bottom soil sampling, respecting the local geology, and processing the data appropriately using geochemical normalisation and exploratory data analysis using ECDF. To obtain reliable results, it is advisable to divide the area into smaller units, and in those units perform high-density sampling to capture spatial concentration patterns in naturally and inevitably heterogeneous real landscapes. Surprisingly, geology can be less important in such deeply human-impacted landscapes as the Ore Mountains. The natural background in the mineralised areas can exceed several times the global or regional backgrounds. Even in geogenically anomalous areas, the ECDF diagrams make it possible to determine the anthropogenic contribution to the total soil contamination. However, it should be taken into account that the distribution of diffuse contamination is not uniform, as it is controlled by vegetation and the terrain topography. The TOP–BOT methodology can be used to estimate the atmospheric deposition of PTE and to determine numerically the impact of the diffuse contamination sources. The total fallout from these sources, estimated via the TOP–BOT methodology applied to soil analyses, is 6 g m^{-2} of Pb and 2 g m^{-2} for As in the Fláje Area, and 5 g m^{-2} for Pb and 2 g m^{-2} for As in the Kovářská Area. The methodology demonstrated in this work could be used to establish a map of ancient emission sources for the Ore Mountains, yet missing.

Author Contributions: Conceptualization, M.H. and T.M.G.; methodology, M.H., P.P., M.Š. and T.M.G.; software, M.H., P.P. and M.Š.; formal analysis, M.H. and T.M.G.; investigation, M.H. and T.M.G.; resources, M.H.; writing—original draft preparation, M.H. and T.M.G.; writing—review and editing, M.H. and T.M.G.; visualization, M.H. and Š.T.; supervision, T.M.G.; project administration, M.H.; funding acquisition, M.H. All authors have read and agreed to the published version of the manuscript.

Funding: This research was funded by SGS (UJEP-SGS-44202/15/2084/01) in UJEP Ústí nad Labem.

Data Availability Statement: The original contributions presented in the study are included in the article, further inquiries can be directed to the corresponding author.

Acknowledgments: The authors would like to thank M. Maříková and P. Vorm from the Institute of Inorganic Chemistry in Řež for the laboratory processing of samples and XRF analysis. We are thankful to S. Draganchev for his help in fieldwork. We also thank J. Elznicová for her advice about GIS.

Conflicts of Interest: The authors declare no conflicts of interest. The funders had no role in the design of the study; in the collection, analyses, or interpretation of data; in the writing of the manuscript; or in the decision to publish the results.

References

1. Ander, E.L.; Johnson, C.C.; Cave, M.R.; Palumbo-Roe, B.; Nathanail, C.P.; Lark, R.M. Methodology for the determination of normal background concentrations of contaminants in English soil. *Sci. Total Environ.* **2013**, *454–455*, 604–618. [CrossRef]
2. Vácha, R.; Skála, J.; Čechmánková, J.; Horváthová, V.; Hladík, J. Toxic elements and persistent organic pollutants derived from industrial emissions in agricultural soils of the Northern Czech Republic. *J. Soils Sed.* **2015**, *15*, 1813–1824. [CrossRef]
3. Reimann, C.; Fabian, K.; Flem, B.; Andersson, M.; Filzmoser, P.; Englmaier, P. Geosphere-biosphere circulation of chemical elements in soil and plant systems from a 100 km transect from southern central Norway. *Sci. Total Environ.* **2018**, *639*, 129–145. [CrossRef] [PubMed]
4. Gosar, M.; Šajn, R.; Bavec, Š.; Gaberšek, M.; Pezdir, V.; Miler, M. Geochemical background and threshold for 47 chemical elements in Slovenian topsoil. *Geologija* **2019**, *62*, 5–57. [CrossRef]
5. Pasieczna, A.; Konon, A.; Nadłonek, W. Sources of anthropogenic contamination of soil in the Upper Silesian Agglomeration (southern Poland). *Geol. Q.* **2020**, *64*, 988–1003. [CrossRef]
6. Kelepertzis, E.; Stathopoulou, E. Availability of geogenic heavy metals in soils of Thiva town (central Greece). *Environ. Monit. Assess.* **2013**, *185*, 9603–9618. [CrossRef]
7. Zhang, H.; Luo, Y.; Teng, Y.; Wan, H. PCB contamination in soils of the Pearl River Delta, South China: Levels, sources, and potential risks. *Environ. Sci. Pollut. Res.* **2013**, *20*, 5150–5159. [CrossRef] [PubMed]
8. Amorosi, A.; Guermandi, M.; Marchi, N.; Sammartino, I. Fingerprinting sedimentary and soil units by their natural metal contents: A new approach to assess metal contamination. *Sci. Total Environ.* **2014**, *500–501*, 361–372. [CrossRef]
9. dos Santos, L.M.R.; Gloaguen, T.V.; de Souza Fadigas, F.; Chaves, J.M.; Martins, T.M.O. Metal accumulation in soils derived from volcano-sedimentary rocks, Rio Itapicuru Greenstone Belt, northeastern Brazil. *Sci. Total Environ.* **2017**, *601–602*, 1762–1774. [CrossRef]
10. Zhang, L.; McKinley, J.; Cooper, M.; Peng, M.; Wang, Q.; Song, Y.; Cheng, H. A regional soil and river sediment geochemical study in Baoshan area, Yunnan province, southwest China. *J. Geochem. Explor.* **2020**, *217*, 106557. [CrossRef]
11. Kafka, J. *Rudné a Uranové Hornictví České Republiky; [Ore and Uranium Mining in the Czech Republic]*; DIAMO: Rožná, Czech Republic, 2003; p. 647. ISBN 80-86331-67-9.
12. Bohdálková, L.; Bohdálek, P.; Břízová, E.; Pacherová, P.; Kuběna, A.A. Atmospheric metal pollution records in the Kovářská Bog (Czech Republic) as an indicator of anthropogenic activities over the last three millennia. *Sci. Total Environ.* **2018**, *633*, 857–874. [CrossRef]
13. Tolksdorf, J.F.; Kaiser, K.; Petr, L.; Herbig, C.; Kočár, P.; Heinrich, S.; Wilke, F.D.H.; Theuerkauf, M.; Fülling, A.; Schubert, M.; et al. Past human impact in a mountain forest: Geoarchaeology of a medieval glass production and charcoal hearth site in the Erzgebirge, Germany. *Reg. Environ. Chang.* **2020**, *20*, 71. [CrossRef]
14. Tarvainen, T.; Reichel, S.; Müller, I.; Jordan, I.; Hube, D.; Eurola, M.; Loukola-Ruskeeniemi, K. Arsenic in agro-ecosystems under anthropogenic pressure in Germany and France compared to a geogenic As region in Finland. *J. Geochem. Explor.* **2020**, *217*, 106606. [CrossRef]
15. Beier, T.; Opp, C.; Hahn, J.; Zitzer, N. Sink and Source Functions for Metal(loid)s in Sediments and Soils of Two Water Reservoirs of the Ore Mountains, Saxony, Germany. *Appl. Sci.* **2022**, *12*, 6354. [CrossRef]
16. Goldschmidt, V.M. The principles of distribution of chemical elements in minerals and rocks. *J. Chem. Soc. Lond.* **1937**, 655–673.
17. Fabian, K.; Reimann, C.; de Caritat, P. Quantifying diffuse contamination: Method and application to Pb in soil. *Environ. Sci. Technol.* **2017**, *51*, 6719–6726. [CrossRef] [PubMed]
18. Matys Grygar, T.; Elznicová, J.; Tůmová, Š.; Kylich, T.; Skála, J.; Hron, K.; Álvarez Vázquez, M.Á. Moving from geochemical to contamination maps using incomplete chemical information from long-term high-density monitoring of Czech agricultural soils. Environ. *Earth Sci.* **2023**, *82*, 6. [CrossRef]
19. Baize, D.; Sterckeman, T. Of the necessity of knowledge of the natural pedo-geochemical background content in the evaluation of the contamination of soils by trace elements. *Sci. Total Environ.* **2001**, *264*, 127–139. [CrossRef] [PubMed]
20. Wang, H.; Yilihamu, Q.; Yuan, M.; Bai, H.; Xu, H.; Wu, J. Prediction models of soil heavy metal(loid)s concentration for agricultural land in Dongli: A comparison of regression and random forest. *Ecol. Indic.* **2020**, *119*, 106801. [CrossRef]
21. Boente, C.; Baragaño, D.; García-González, N.; Forján, R.; Colina, A.; Gallego, J.R. A holistic methodology to study geochemical and geomorphological control of the distribution of potentially toxic elements in soil. *Catena* **2022**, *208*, 105730. [CrossRef]
22. Ribeiro, M.T.; Guestrin, C. "Why Should I Trust You?" Explaining the Predictions of Any Classifier. In Proceedings of the 22nd ACM SIGKDD International Conference on Knowledge Discovery and Data Mining, San Francisco, CA, USA, 13–17 August 2016; pp. 1135–1144.

23. Zhao, Z.; Qiao, K.; Liu, Y.; Chen, J.; Li, C. Geochemical Data Mining by Integrated Multivariate Component Data Analysis: The Heilongjiang Duobaoshan Area (China) Case Study. *Minerals* **2022**, *12*, 1035. [CrossRef]
24. Sarti, G.; Sammartino, I.; Amorosi, A. Geochemical anomalies of potentially hazardous elements reflect catchment geology: An example from the Tyrrhenian coast of Italy. *Sci. Total Environ.* **2020**, *714*, 136870. [CrossRef]
25. Lienard, A.; Colinet, G. Assessment of vertical contamination of Cd, Pb, and Zn in soils around a former ore smelter in Wallonia, Belgium. *Environ. Earth Sci.* **2016**, *75*, 1322. [CrossRef]
26. Reimann, C.; Fabian, K.; Birke, M.; Filzmoser, P.; Demetriades, A.; Négrel, P.; Oorts, K.; Matschullat, J.; de Caritat, P.; Albanese, S.; et al. GEMAS: Establishing geochemical background and threshold for 53 chemical elements in European agricultural soil. *Appl. Geochem.* **2018**, *88*, 730–740. [CrossRef]
27. Spahić, M.P.; Sakan, S.; Cvetković, Ž.; Tančić, P.; Trifković, J.; Nikić, Z.; Manojlović, D. Assessment of contamination, environmental risk, and origin of heavy metals in soils surrounding industrial facilities in Vojvodina, Serbia. *Environ. Monit. Assess.* **2018**, *190*, 208. [CrossRef] [PubMed]
28. Sinclair, A.J. *Applications of Probability Graphs in Mineral Exploration*; Special Volume No. 4; The Association of Exploration Geochemists: Nepean, ON, Canada; Richmond Printers: Richmond, BC, Canada, 1976.
29. Reimann, C.; Fabian, K.; Flem, B. Cadmium enrichment in topsoil: Separating diffuse contamination from biosphere-circulation signals. *Sci. Total Environ.* **2019**, *651*, 1344–1355. [CrossRef] [PubMed]
30. Reimann, C.; Fabian, K.; Flem, B.; Englmaier, P. The large-scale distribution of Cu and Zn in sub- and topsoil: Separating topsoil bioaccumulation and natural matrix effects from diffuse and regional contamination. *Sci. Total Environ.* **2019**, *655*, 730–740. [CrossRef]
31. Flem, B.; Acosta-Gongora, P.; Andersson, M.; Finne, T.E.; Minde, Å. *Organic Soil Geochemistry in Southern Trøndelag, QC—Report*; Report No: 2021.006; Geological Survey of Norway: Trondheim, Norway, 2021.
32. Giandon, P. Soil Contamination by Diffuse Inputs. In *Environmental Indicators*; Springer: Dordrecht, The Netherlands, 2015; ISBN 978-94-017-9498-5. [CrossRef]
33. Vilímek, V.; Raška, P. The Krušné Hory Mts.—The Longest Mountain Range of the Czech Republic. In *Landscapes and Landforms of the Czech Republic*; Geomorphological Landscapes; Springer: Cham, Switzerland, 2016. [CrossRef]
34. UNESCO World Heritage Site. Available online: http://www.montanregion.cz/cs/montanregion.html (accessed on 20 October 2023).
35. Kaiser, K.; Theuerkauf, M.; Hieke, F. Holocene forest and land-use history of the Erzgebirge, central Europe: A review of palynological data. *E G Quat. Sci. J.* **2023**, *72*, 127–161. [CrossRef]
36. Tolksdorf, J.F.; Schröder, F.; Petr, L.; Herbig, C.; Kaiser, K.; Kočár, P.; Fülling, A.; Heinrich, S.; Hönig, H.; Hemker, C. Evidence for Bronze Age and Medieval tin placer mining in the Erzgebirge mountains, Saxony (Germany). *Geoarchaeology* **2019**, *35*, 2. [CrossRef]
37. Cílová, Z.; Woitsch, J. Potash—A key raw material of glass batch for Bohemian glasses from 14th–17th centuries? *J. Archaeol. Sci.* **2012**, *39*, 371–380. [CrossRef]
38. Černá, E.; Frýda, F. Sklo vrcholného středověku—Současný stav a perspektivy studia historických (Glass of the High Middle Ages—Current state and perspectives of historical studies Technologies). *Archaeol. Hist.* **2000**, *35*, 355–357.
39. Botula, Y.D.; Nemes, A.; Van Ranst, E.; Mafuka, P.; De Pue, J.; Cornelis, W.M. Hierarchical pedotransfer functions to predict bulk density of highly weathered soils in Central Africa. *Soil Sci. Soc. Am.* **2015**, *79*, 476–486. [CrossRef]
40. Geological Map 1:50,000. Praha: Czech Geological Survey. Available online: https://mapy.geology.cz/geocr50/ (accessed on 10 October 2023).
41. Adamec, S.; Tůmová, Š.; Hošek, M.; Lučić, M.; Matys Grygar, T. Pitfalls of distinguishing anthropogenic and geogenic reasons for risk elements in soils around coal-fired power plant: From case study in NW Czech Republic to general recommendations. *J. Soils Sed.* 2024. [CrossRef]
42. Álvarez-Vázquez, M.Á.; Hošek, M.; Elznicová, J.; Pacina, J.; Hron, K.; Fačevicová, K.; Talská, R.; Bábek, O.; Grygar, T.M. Separation of geochemical signals in fluvial sediments: New approaches to grain-size control and anthropogenic contamination. *Appl. Geochem.* **2020**, *123*, 104791. [CrossRef]
43. Sterckeman, T.; Douay, F.; Baize, D.; Fourrier, H.; Proix, N.; Schvartz, C. Trace elements in soils developed in sedimentary materials from Northern France. *Geoderma* **2006**, *136*, 912–929. [CrossRef]
44. Bábek, O.; Grygar, T.M.; Faměra, M.; Hron, K.; Nováková, T.; Sedláček, J. Geochemical background in polluted river sediments: How to separate the effects of sediment provenance and grain size with statistical rigour? *Catena* **2015**, *135*, 240–253. [CrossRef]
45. Dung, T.T.T.; Cappuyns, V.; Swennen, R.; Phung, N.K. From geochemical background determination to pollution assessment of heavy metals in sediments and soils. *Rev. Environ. Sci. Biotechnol.* **2013**, *12*, 335–353. [CrossRef]
46. Matys Grygar, T.; Popelka, J. Revisiting geochemical methods of distinguishing natural concentrations and pollution by risk elements in fluvial sediments. *J. Geochem. Explor.* **2016**, *170*, 39–57. [CrossRef]
47. Goldschmidt, V.M. *Geochemistry*; Muir, A., Ed.; Clarendon Press: Oxford, UK, 1954.
48. Reimann, C.; Filzmoser, P.; Garrett, R.G.; Dutter, R. *Statistical Data Analysis Explained: Applied Environmental Statistics with R*; John Wiley & Sons: Chichester, UK, 2008; ISBN 978-0-470-98581-6.
49. Reimann, C.; Fabian, K. Quantifying diffuse contamination: Comparing silver and mercury in organogenic and minerogenic soil. *Sci. Total Environ.* **2022**, *832*, 155065. [CrossRef]

50. Flem, B.; Reimann, C.; Fabian, K. Excess Cr and Ni in top soil: Comparing the effect of geology, diffuse contamination, and biogenic influence. *Sci. Total Environ.* **2022**, *843*, 157059. [CrossRef]
51. Rudnick, R.L.; Gao, S. Treatise on Geochemistry: Composition of the continental crust. In *The Crust: Treatise on Geochemistry*; Rudnick, R.L., Holland, H.D., Turekian, K.K., Eds.; Elsevier-Pergamon: Oxford, UK, 2003; Volume 3, pp. 1–64.
52. Salminen, R.; Batista, M.J.; Bidovec, M.; Demetriades, A.; De Vivo, B.; De Vos, W.; Duris, M.; Gilucis, A.; Gregorauskiene, V.; Halamic, J.; et al. *Geochemical Atlas of Europe. Part 1—Background Information, Methodology and Maps*; Geological Survey of Finland: Espoo, Finland, 2005; ISBN 951-690-921-3.
53. Ministry of Environment of Czech Republic (2016): Decree No. 153/2016 Coll., about the Agricultural Soil Quality and Protection Requirements. Legal Code of the Czech Republic; pp. 2692–2699. (In Czech). Available online: https://www.e-sbirka.cz/sb/2016/153?zalozka=text (accessed on 20 November 2023).
54. Reimann, C.; Garret, R.G. Geochemical background—Concept and reality. *Sci. Total Environ.* **2005**, *350*, 12–27. [CrossRef]
55. O'Shea, B.; Stransky, M.; Leitheiser, S.; Brock, P.; Marvinney, R.; Zheng, Y. Heterogeneous arsenic enrichment in meta-sedimentary rocks in central Maine, United States. *Sci. Total Environ.* **2015**, *505*, 1308–1319. [CrossRef]
56. Goldhaber, S.B. Trace element risk assessment: Essentiality vs. toxicity. *Regul. Toxic. Pharmacol.* **2003**, *38*, 232–242. [CrossRef]
57. Wang, X.; Han, Z.; Wang, W.; Zhang, B.; Wu, H.; Nie, L.; Zhou, J.; Chi, Q.; Xu, S.; Liu, H.; et al. Continental-scale geochemical survey of lead (Pb) in mainland China's pedosphere: Concentration, spatial distribution and influences. *Appl. Geochem.* **2018**, *100*, 55–63. [CrossRef]
58. Salminen, R.; Gregorauskiene, V. Considerations regarding the definition of a geochemical baseline of heavy metals in the overburden in areas differing in basic geology. *Appl. Geochem.* **2000**, *15*, 647–653. [CrossRef]
59. Bravo, S.; García-Ordiales, E.; García-Navarro, F.J.; Amorós, J.Á.; Pérez-De-Los-Reyes, C.; Jiménez-Ballesta, R.; Esbrí, J.M.; García-Noguero, E.M.; Higueras, P. Geochemical distribution of major and trace elements in agricultural soils of Castilla-La Mancha (central Spain): Finding criteria for baselines and delimiting regional anomalies. *Environ. Sci. Pollut. Res.* **2023**, *26*, 3100–3114. [CrossRef]
60. Matys Grygar, T.; Faměra, M.; Hošek, M.; Elznicová, J.; Rohovec, J.; Matoušková, Š.; Navrátil, T. Uptake of Cd, Pb, U, and Zn by plants in floodplain pollution hotspots contributes to secondary contamination. *Environ. Sci. Poll. Res.* **2021**, *28*, 51183–51198. [CrossRef] [PubMed]
61. Shotyk, W. Comment on "The biosphere: A homogeniser of Pb-isotope signals" by C. Reimann, B. Flem, A. Arnoldussen, P. Englmaier, T.E. Finne, F. Koller and Ø. Nordgulen. *Appl. Geochem.* **2008**, *23*, 2514–2518. [CrossRef]
62. Density of Materials. SImetric. 2004. Available online: https://www.simetric.co.uk/si_materials.htm (accessed on 10 December 2023).
63. Shotyk, W.; Kempter, H.; Krachler, M.; Zaccone, C. Stable (^{206}Pb, ^{207}Pb, ^{208}Pb) and radioactive (^{210}Pb) lead isotopes in 1 year of growth of sphagnum moss from four ombrotrophic bogs in southern Germany: Geochemical significance and environmental implications. *Geochim. Cosmochim. Acta* **2015**, *163*, 101–125. [CrossRef]
64. Veron, A.; Novak, M.; Brizova, E.; Stepanova, M. Environmental imprints of climate changes and anthropogenic activities in the Ore Mountains of Bohemia (Central Europe) since 13 cal. kyr BP. *Holocene* **2014**, *24*, 919–931. [CrossRef]
65. Windroses at Air Pollution Stations, Praha: Czech Hydrometeorological Institute. Available online: https://www.chmi.cz/files/portal/docs/uoco/isko/tab_roc/2021_enh/pollution_wrose/wrose_UKRUA_GB.html (accessed on 18 December 2023).

Disclaimer/Publisher's Note: The statements, opinions and data contained in all publications are solely those of the individual author(s) and contributor(s) and not of MDPI and/or the editor(s). MDPI and/or the editor(s) disclaim responsibility for any injury to people or property resulting from any ideas, methods, instructions or products referred to in the content.